Extraordinary optical transmission through subwavelength holes in a polaritonic silicon dioxide film

Dye-Zone A. Chen
Department of Mechanical Engineering, Massachusetts Institute of Technology, 77 Massachusetts Avenue, Cambridge, Massachusetts 02139

Rafif Hamam, Marin Soljačić, and John D. Joannopoulos
Department of Physics, Massachusetts Institute of Technology, 77 Massachusetts Avenue, Cambridge, Massachusetts 02139

Gang Chen[a)]
Department of Mechanical Engineering, Massachusetts Institute of Technology, 77 Massachusetts Avenue, Cambridge, Massachusetts 02139

(Received 12 October 2006; accepted 9 April 2007; published online 3 May 2007)

The authors present experimental data showing that extraordinary optical transmission occurs through subwavelength holes etched in an amorphous silicon dioxide film. The discrete frequency ranges of the enhanced transmission suggest the involvement of surface phonon-polaritons in mediating the transmission in a manner analogous to surface plasmons on metal films. Finite-difference time-domain simulations also predict the enhancement and correlate well with the experimental data. Both experimental and theoretical results show a fivefold increase in transmission through a perforated film versus a solid film. © *2007 American Institute of Physics*. [DOI: 10.1063/1.2736267]

The observation of extraordinary optical transmission (EOT) was reported in 1998 by Ebbesen *et al.*.[1] In their experiments, light was normally incident on a metal film which was perforated by subwavelength holes, and the transmission exhibited peak intensities that were much higher than classically predicted. Since this and other observations of EOT,[2–6] there has been significant research in trying to understand the mechanism of the transmission.[7] Depending on the hole diameter, periodicity, and wavelength, there are several possible explanations. These include Fabry-Pérot waveguide resonances,[8] perforated perfect conductors which mimic surface waves,[9,10] and actual surface plasmons, although as has been noted by several authors, the detailed physical mechanism of the transmission is still unclear.[2,11,12]

In this letter we present experimental data demonstrating that EOT also occurs through a perforated dielectric film, where the analogs to surface plasmons are surface phonon-polaritons (SPP). Our results support the thinking that EOT should also be observable with a dielectric film, and point towards SPPs as the mediating mechanism. This idea has been previously suggested,[2] and is being actively studied by other researchers as well.[13]

Unlike surface plasmons which extend from $\omega_p/\sqrt{1+\varepsilon_d}$ down to zero frequency (where ω_p is the plasma frequency and ε_d is the dielectric constant of the surrounding medium), the SPP resonance only occurs over a finite frequency range between the transverse optical and longitudinal optical phonon frequencies where the real part of the dielectric function is negative. Furthermore, for our choice of dielectric material, amorphous silicon dioxide (SiO_2), there are two distinct resonances. One is around 9 μm and the other around 21 μm.[14]

The fabrication of the samples was accomplished via standard microfabrication techniques. The substrates consisted of double-side-polished, 500 μm thick, *p*-type, ⟨100⟩ silicon wafers with 1–10 Ω cm resistivity. The first step was to grow 1 μm of thermal oxide on the silicon wafers. Pattern transfer was achieved using standard contact photolithography. A buffered oxide etch was used to simultaneously remove the back side oxide and etch the desired pattern which consisted of a square lattice of circular holes covering an area of 12×12 mm^2. The lattice constant of the hole arrays was 4 and 8 μm, and the diameter of the holes was 2 μm.

The infrared transmission spectra of the samples were measured using Fourier transform infrared spectroscopy. A Thermo-Nicolet Magna-IR 860 spectrometer was set up with a DTGS/KBr detector and a KBr beam splitter. The detector has a spectral range of 400–4000 cm^{-1} with a resolution of 4 cm^{-1}. Transmission spectra were obtained for normal incidence, and an aperture was used to produce a spot size of 8.75 mm in diameter on the sample.

Shown in Fig. 1 are the measured and the analytically calculated transmission through a 1 μm thick solid film of SiO_2 on a 500 μm thick wafer. The transmission through and reflection from the SiO_2 film alone were calculated using a wave optics formulation. The film was modeled as a thin homogeneous dielectric sandwiched between two infinite half-spaces of vacuum ($\varepsilon=1$) and silicon ($\varepsilon=11.7$), resulting in the transmissivity $T_{\mathrm{film}}(\omega)$, and reflectivity $R_{\mathrm{film}}(\omega)$ of the film alone.[15] On the other side of the wafer next to air, Fresnel coefficients were used to calculate the corresponding quantities, $T_{\mathrm{back}}(\omega)$ and $R_{\mathrm{back}}(\omega)$. Ray tracing of the intensity through the substrate is then used to calculate the transmission through the entire structure.[14] Absorption in the silicon wafer, $A_{\mathrm{silicon}}(\omega)=\exp(-4\pi\kappa d/\lambda)$, where κ is the imaginary part of the complex index of refraction, d is the thickness of the wafer, and λ is the wavelength, was significant due to the

[a)]Electronic mail: gchen2@mit.edu

 © 2007 American Institute of Physics
Downloaded 05 May 2007 to 18.251.7.37. Redistribution subject to AIP license or copyright, see http://apl.aip.org/apl/copyright.jsp

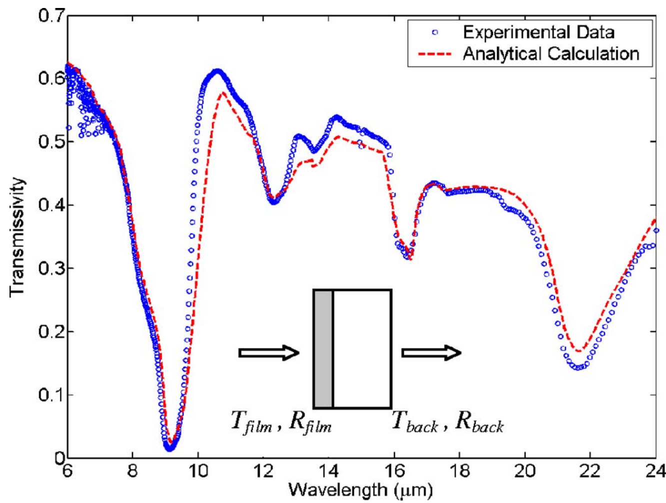

FIG. 1. (Color online) Measured and analytically calculated transmission spectra of a 1 μm thick film of silicon dioxide on a 500 μm thick silicon wafer. The inset shows a side view of the light path through the sample and the definition of the transmissivities and reflectivities.

large thickness and was also included. Thus, the overall transmission is given by

$$T_{\text{overall}}(\omega) = \frac{T_{\text{film}}(\omega)T_{\text{back}}(\omega)}{1 - R_{\text{film}}(\omega)R_{\text{back}}(\omega)}A_{\text{silicon}}(\omega). \quad (1)$$

The optical constants used in these calculations were taken from published values.[14] Overall, there is very good agreement between the calculated and measured spectra. The gross features of the spectrum are clearly reproduced, as is much of the small scale structure. The small discrepancy between the measured and calculated spectra is likely due to the fact that the actual optical constants depend on the doping level of the silicon.[16,17]

Numerical simulations were performed using a finite-difference time-domain (FDTD) algorithm.[18] Apart from discretization, these simulations model Maxwell's equations in three dimensions exactly, taking into account both material dispersion and absorption. As shown in the inset of Fig. 2(b), the computational cell used had dimensions of $a \times a \times 250$ grid points (GP), where a is the lattice constant (in GP) of the hole period, and every GP corresponds to 0.1 μm. The SiO_2 film was placed in the middle of the computational cell, and was surrounded by vacuum on one side, and a half space of silicon on the other. Absorption and dispersion in the SiO_2 film were incorporated by means of a Lorentz model for the dielectric function,

$$\varepsilon(\omega) = \varepsilon_\infty + \sum_{j=1}^{2} \frac{\sigma_j}{\omega_{0,j}^2 - \omega^2 - i\omega\gamma_j}, \quad (2)$$

where i is equal to $\sqrt{-1}$, ω is the angular frequency, ε_∞ is the high-frequency dielectric constant, $\omega_{0,j}$ is the resonance absorption frequency, γ_j is the linewidth due to damping, and σ_j is the conductivity. These coefficients were obtained by fitting the actual ε values[14] for SiO_2 to the above equation, and are given by $\varepsilon_\infty = 2.0014$, $\sigma_1 = 4.4767 \times 10^{27}$ rad^2/s^2, $\omega_{0,1} = 8.6732 \times 10^{13}$ rad/s, $\gamma_1 = 3.3026 \times 10^{12}$ rad/s, $\sigma_2 = 2.3584 \times 10^{28}$ rad^2/s^2, $\omega_{0,2} = 2.0219 \times 10^{14}$ rad/s, and $\gamma_2 = 8.3983 \times 10^{12}$ rad/s. A temporally Gaussian pulse was incident normally on the SiO_2 film from the vacuum side. Perfectly matched layer[19,20] (PML) boundary conditions were applied on the boundaries normal to the incident light to prevent reflections, and periodic boundary conditions were applied in the other directions.

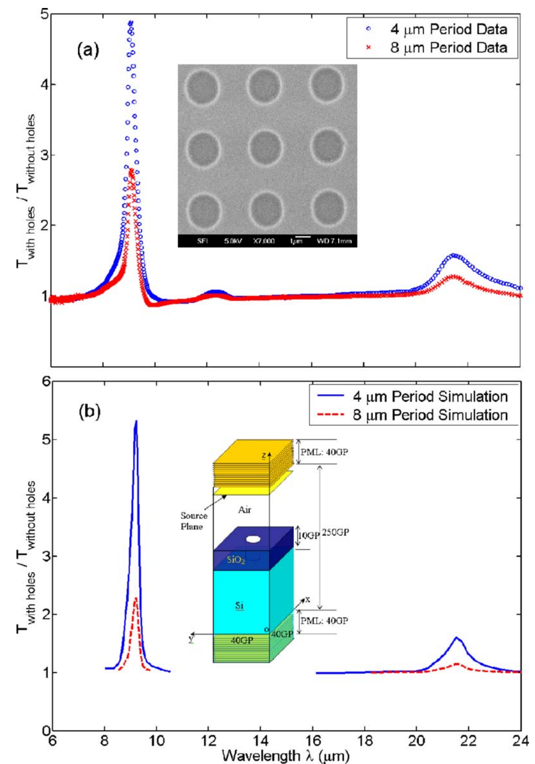

FIG. 2. (Color online) Transmission through silicon dioxide films perforated with 2 μm holes normalized to the transmission through a solid film. (a) The experimentally measured transmission spectra. The inset shows a scanning electron micrograph of the actual sample. (b) FDTD simulation results for the same structures. The inset shows a schematic of the computational cell for the structure with a 4 μm period.

The electromagnetic fields at planes located on both sides of the film just before the PMLs were recorded. Then, the Poynting power fluxes were calculated from the discrete Fourier transforms of the fields. However, this power then needs to be normalized to the incident flux. Thus, the simulation was repeated with vacuum only in the computational cell, and the fluxes were recorded again. The transmissivity, $T_{\text{film}}(\omega)$, is given by the ratio of the flux through the plane with the structure, over the flux through the same plane, but in the case where there is only vacuum. The calculation for the reflectivity $R_{\text{film}}(\omega)$ is similar, although in this case the incident and reflected fields need to be separated before calculating the flux. The same procedure and calculations were also repeated for the perforated SiO_2 films.

Plotted in Fig. 2(a) are the experimentally measured transmission spectra of a perforated SiO_2 film normalized to the transmission through a solid film. Thus, a value greater than unity indicates that the transmission through the perforated film is more than that through the solid film. In the range of wavelengths from 6 to 24 μm, the 2 μm holes are clearly below the cutoff wavelength and do not support any propagating modes. Thus, for most of the range the transmission ratio is unity as is expected. Nevertheless, it is observed that the perforated film has significantly greater transmission in two regions: one around 9 μm and the other around 21 μm. Furthermore, as seen in Fig. 2(b), the FDTD simulations also predict enhanced transmission of similar magnitude and at the same frequencies as the experimental data.

Downloaded 05 May 2007 to 18.251.7.37. Redistribution subject to AIP license or copyright, see http://apl.aip.org/apl/copyright.jsp

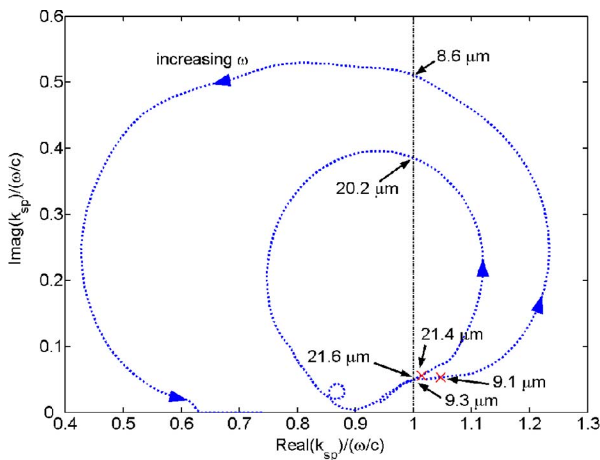

FIG. 3. (Color online) Complex plot of the surface phonon-polariton wave vector at an interface of amorphous silicon dioxide and air. The wavelengths of the peak EOT transmission are indicated at 9.1 and 21.4 μm.

Due to the highly damped nature of the SiO_2 phonon resonances, the criterion for the existence of the SPPs is not as simple as the oft-quoted $\varepsilon_1 = -\varepsilon_2$ where ε_1 and ε_2 are the dielectric functions of the materials on either side of the interface and are real quantities.[21] Rather, solutions of the complex dispersion relation pinpoint at which frequencies the surface modes exist. Although the dispersion relation will be modified by the array of holes, it has been noted that the effect will be to lower the frequency of the existing modes,[9] and the magnitude of such redshifts have been observed to be small.[22,23] As such, we consider the dispersion relation at a smooth interface for simplicity. This is given by $k_{sp} = (\omega/c)\sqrt{\varepsilon_{SiO_2}\varepsilon_2/(\varepsilon_{SiO_2}+\varepsilon_2)}$, where k_{sp} is the in-plane wave vector, c is the speed of light, ε_{SiO_2} is the dielectric function of SiO_2, and ε_2 is the dielectric function of vacuum. Assuming a real frequency, a complex wave vector is found where the imaginary part of the wave vector gives the attenuation of the mode.[24,25]

Shown in Fig. 3 is a complex plot of the wave vector k_{sp} which has been normalized to the light line in vacuum. The contour is generated by plotting the real and imaginary parts of the wave vector at each frequency. It is seen that there are two frequency ranges (8.6–9.3 and 20.2–21.6 μm) where the real part of the wave vector is greater than the light line. Hence, these modes are nonradiating. Furthermore, there are portions of these ranges where the imaginary part of the wave vector is small, which indicates that the damping is low. Together, these two characteristics indicate the existence of SPPs. Also plotted are the wavelengths where the peak EOT occurs, at 9.1 μm and 21.4 μm. It is seen that these wavelengths clearly fall in the range of these SPPs.

It could be argued that the transmission enhancement is due to a reduction in the effective refractive index of the film caused by the holes. However, this mechanism would increase the transmission over the entire spectrum, which is clearly not the case. Rather, the fact that EOT is only observed at the frequencies where SPPs exist strongly points towards their involvement in the transmission. Coupling of the normally incident light to the surface modes on the air-SiO_2 interface is via the grating momentum provided by the hole array.[23] After some type of resonant interaction in the perforated film, the lack of a surface mode at the SiO_2-silicon interface then allows for the resonant mode to couple directly back into a propagating wave in the silicon substrate.

In summary, we have presented experimental verification of extraordinary optical transmission through a dielectric film. The frequencies where EOT is observed correspond very well with the frequencies where SPPs are found to exist. Further experiments with unsupported dielectric films and varied hole diameter could further elucidate the mechanisms of transmission.

The authors would like to thank Arvind Narayanaswamy and Jorge Bravo-Abad for many helpful and insightful discussions, and C. Thomas Harris for providing the scanning electron microscopy images. This work was supported by the DOE (Contract No. DE-FG02-02ER45977) and a DOD/ONR MURI (Grant No. N00014-01-1-0803). This material is based upon work supported by the National Science Foundation under the following NSF programs: Partnerships for Advanced Computational Infrastructure; Distributed Terascale Facility (DFT); and Terascale Extensions: Enhancements to the Extensible Terascale Facility.

[1] T. W. Ebbesen, H. J. Lezec, H. F. Ghaemi, T. Thio, and P. A. Wolff, Nature (London) **391**, 667 (1998).
[2] W. L. Barnes, W. A. Murray, J. Dintinger, E. Devaux, and T. W. Ebbesen, Phys. Rev. Lett. **92**, 107401 (2004).
[3] H. F. Ghaemi, T. Thio, D. E. Grupp, T. W. Ebbesen, and H. J. Lezec, Phys. Rev. B **58**, 6779 (1998).
[4] D. E. Grupp, H. J. Lezec, T. W. Ebbesen, K. M. Pellerin, and T. Thio, Appl. Phys. Lett. **77**, 1569 (2000).
[5] T. J. Kim, T. Thio, T. W. Ebbesen, D. E. Grupp, and H. J. Lezec, Opt. Lett. **24**, 256 (1999).
[6] T. Thio, H. F. Ghaemi, H. J. Lezec, P. A. Wolff, and T. W. Ebbesen, J. Opt. Soc. Am. B **16**, 1743 (1999).
[7] J. Bravo-Abad, F. J. García-Vidal, and L. Martín-Moreno, Phys. Rev. Lett. **93**, 227401 (2004).
[8] D. L. C. Chan, M. Soljacic, and J. D. Joannopoulos, Phys. Rev. E **74**, 016609 (2006).
[9] J. B. Pendry, L. Martín-Moreno, and F. J. Garcia-Vidal, Science **305**, 847 (2004).
[10] F. J. Garcia-Vidal, L. Martín-Moreno, and J. B. Pendry, J. Opt. A, Pure Appl. Opt. **7**, S97 (2005).
[11] W. Fan, S. Zhang, B. Minhas, K. J. Malloy, and S. R. J. Brueck, Phys. Rev. Lett. **94**, 033902 (2005).
[12] L. Martín-Moreno, F. J. García-Vidal, H. J. Lezec, K. M. Pellerin, T. Thio, J. B. Pendry, and T. W. Ebbesen, Phys. Rev. Lett. **86**, 1114 (2001).
[13] D. Korobkin, Y. Urzhumov, B. Neuner, III, G. Shvets, Z. Zhang, and I. D. Mayergoyz, e-print physics/0606207 (2006).
[14] E. D. Palik, *Handbook of Optical Constants of Solids* (Academic Press, Orlando, 1985), Vol. 1, p. 587.
[15] M. Born and E. Wolf, *Principles of Optics*, 7th (expanded) ed. (Cambridge University Press, New York, 1999), p. 65.
[16] B. Lojek, International Conference on Advanced Thermal Processing of Semiconductors, 23–26 September, 2003 Charleston, NC (IEEE, Piscataway, NJ, 2003).
[17] Y. Laghla and E. Scheid, Thin Solid Films **306**, 67 (1997).
[18] A. Taflove and S. C. Hagness, *Computational Electrodynamics: The Finite-Difference Time-Domain Method*, 3rd ed. (Artech House, Norwood, MA, 2000), p. 15.
[19] P. Lalanne and E. Silberstein, Opt. Lett. **25**, 1092 (2000).
[20] E. Silberstein, P. Lalanne, J.-P. Hugonin, and Q. Cao, J. Opt. Soc. Am. A **18**, 2865 (2001).
[21] H. Raether, *Surface Plasmons on Smooth and Rough Surfaces and on Gratings* (Springer, Berlin, 1988), p. 5.
[22] C. Genet, M. P. v. Exter, and J. P. Woerdman, Opt. Commun. **225**, 331 (2003).
[23] C. Genet and T. W. Ebbesen, Nature (London) **445**, 39 (2007).
[24] J. B. Pendry, *Low Energy Electron Diffraction* (Academic, New York, 1974), p. 92.
[25] M. Fukui, V. C. Y. So, and R. Normandin, Phys. Status Solidi B **91**, K61 (1979).

Downloaded 05 May 2007 to 18.251.7.37. Redistribution subject to AIP license or copyright, see http://apl.aip.org/apl/copyright.jsp